

Observers and Feedback Control for Shear Layer Vortices

Mark Pastoor, Rudibert King

Measurement and Control Group,
Institute for Process and Plant Technology
Berlin University of Technology
Straße des 17 Juni 135
D-10623 Berlin, Germany
mark.pastoor@tu-berlin.de
rudibert.king@tu-berlin.de

Bernd R. Noack

Hermann-Föttinger-Institute
of Fluid Mechanics
Berlin University of Technology
Straße des 17 Juni 135
D-10623 Berlin, Germany
Bernd.R.Noack@tu-berlin.de

Gilead Tadmor

Electrical & Computer
Engineering Department
Northeastern University
440 Dana Research Building
Boston, MA 02115, U.S.A.
tadmor@ece.neu.edu

Abstract—The stirring motion of shear layer vortices plays a prominent and often critical role in diverse engineering applications. Periodic zero net flow actuation is an established mechanism to effect shear layer instability and growth. Active feedback control is considered here as a means to regulate and maximize shear layer mixing: Feedback utilizes estimated vortex locations to harmonize actuation with vortex release. We propose an observer structure based on a phenomenological dynamic phasor model for the travelling waveform of sensors' readings, and illustrate its use in simulations and open and closed loop experiments with the backward facing step system, and in free shear layer simulations.

I. INTRODUCTION

Shear flows occur due to significant mean fluid velocity changes, such as behind bluff bodies, airfoils and corners. Vortical structures interact and aggregate, forming larger coherent structures [1] whose stirring motion is an efficient mixing mechanism [2]–[5]. Shear layer mixing plays a prominent and often critical role in engineering applications, including aircraft, automotive, imaging, air conditioning, the chemical and bioreactor industry, and turbine engines, to name a few. The potential economic, technological and environmental implications of viable methods to regulate these mechanisms are enormous. The ability to actuate unsteady shear layers (e.g., by synthetic jets, plasma actuators, MEMs & fuel control), to generate or suppress mixing, has been demonstrated experimentally and in dynamical systems studies. Most past flow control studies concentrated on passive & open loop actuation. The introduction of feedback (see e.g. the books & reviews [6]–[10]) is a relatively new undertaking, aiming at substantial performance improvements and, in some cases, as a critical enabler.

A major hurdle for the feasibility of *model-based* feedback design for *real time* implementation is the complexity of a distributed, highly sensitive, nonlinear system, and its first principles model, the Navier-Stokes equations (NSE). Design oriented models are thus bound to focus on the dynamics of a low order parametrization of some coherent structures in the

flow. Common examples include very low order vortex models [11]–[16] and very low order Galerkin models [17], [18].

Here we focus on a yet simpler modeling framework, exploiting the flip side of a generic restriction of feasible control to slow manipulation of phase in nearly periodic actuators, such as pulsating synthetic jets: A key control objective, in such cases, is to regulate the phase difference between the actuator and a meaningful concept of the “phase” of the flow; a satisfactory model is then one that is useful for dynamic estimation of the phase in a nearly periodic flow. We propose a modeling framework that is focused on the representation of sensor signals in terms of travelling waveforms with slowly varying Fourier coefficients (also known as *dynamic phasors* [19], [20]), which are the subject of dynamic estimation. Following our preliminary results in [21], [22], this article examines the development of such models and their application to feedback, in two generic flow configurations: The free shear layer in an ideal two dimensional flow, and the shear layer behind a backward facing step. Designs are tested in both simulation models and in an experimental testbed for the backward facing step, demonstrating both the capability of the suggested observer design framework, and its utilization as a means to feedback regulate shear layer dynamics.

II. THE SYSTEM AND DESIGN OBJECTIVES

Shear layer flows are unstable and sensitive to periodic perturbations [23]–[25], a phenomenon known as *Kelvin-Helmholtz* instability. The instability is manifest by the periodic release of vortices that convect and grow along the shear layer, undergo a series of pairwise merging into larger and larger structures, and eventually dissipate into the flow. Periodic excitation of upstream perturbations at the natural frequency is an effective means to enhance mixing [26] and it tends to reduce aperiodic modulations, typical of the natural flow. This harmonization effects is desirable in its own right, under a mixing objective, as it reduces the attenuating effect of out-of-phase waveforms.

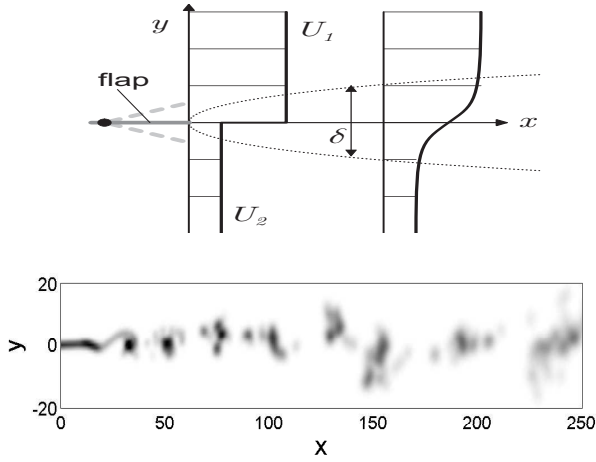


Fig. 1. Top: A schematic of the free shear layer with a flap actuator. Bottom: Visualization of vorticity distribution.

A. The free shear layer

The two dimensional free shear layer is an idealization of systems such as the wake behind a thin airfoil, where no boundary interactions occur past the inception of the shear layer. A schematic is depicted at the top of Figure 1, featuring the discrepancy between the incoming flow velocities above and below a separating wall, and the growth of the of the shear layer as it evolves, downstream. Both Kelvin-Helmholtz vortices and vortex pairing are apparent in the shear layer visualization at the bottom plot of Figure 1. The flow velocity along the shear layer is the average of the two input velocities, and shear layer vortices convect at that velocity, creating a simple relation between the vortex generation frequency and the spatial wave length (i.e., the average distance between vortices in the near field). A natural instability determines a peak sensitivity at a characteristic frequency, but the flow is sensitive to disturbances at a range of frequencies, a fact that is reflected by seemingly random drifts in the upstream periodic behavior as well as aperiodic vortex pairing, further downstream.

For rapid prototyping and observer proof of concept we use a moderate order simulation vortex model. Its main parameters are: Incoming flow velocities of $U_1 = 1.5$, $U_2 = .5$, hence a shear layer velocity of $U_s = 0.5(U_1 + U_2) = 1$. The initial vortex core radius, defining the characteristic length, is $R = 1$ and the circulation production rate is $dG/dt = -1$. The Strouhal number (i.e., the natural instability frequency, normalized by the characteristic length and period) is $St = fR/U = 0.05$, leading to a frequency of $\omega = 0.1\pi$, time period $T = 20$ and spatial wave length $\lambda = 20$. Periodic actuation at the instability frequency is represented by an oscillating flap at the end of the separating wall (Figure 1, top). The flap length is $\lambda = 20$ and the vertical oscillation stroke is 0.05λ .

Random perturbations and drift in the periodic behavior will be a challenge in observer design, where the objective is the estimation of the center location of vortical structures from data obtained from an array of sensors. As will be seen in the backward step benchmark, this information can be used to

further harmonize vortex release, enhance shear layer growth and increase its mixing effect. Locating vortex position can also be used in a control aiming to enhance or delay vortex merging by local actuation at a specific location along the shear layer [12], [22], [27]. Here we shall only discuss the dynamic estimation component. In that context we postulate measurements of the stream-wise fluid velocity at 24 points along the line $y = -15$ (relative to Figure 1). Velocity sensors were selected due to the relative ease to incorporate them in the vortex model we use to test the suggested framework, but the proposed estimation framework is equally applicable to more practical alternatives, such as pressure gages, as is done in the experimental setup used in our next benchmark, in §II-B.

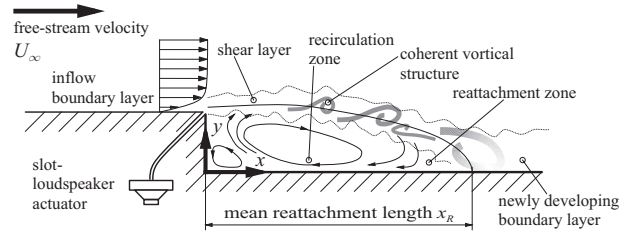


Fig. 2. Flow field downstream of a backward-facing step: Top: A schematic of our experimental testbed. Bottom: A detailed 3D Large Eddy) simulation from [28]

B. The flow over a backward facing step

Observer and feedback development for the backward facing step benchmark are tested in an experimental setup which is schematically sketched in Fig. 2, along with simulation based visualization of the flow. The flow detaches at the step and reattaches downstream. The wake area of current interest comprises a recirculation bubble bounded by a shear layer and a reattachment zone. Sinusoidal zero net flow actuation through a slot at the corner is effected by a loudspeaker, allowing for slow modulation of actuation amplitude and phase. The reattachment point is determined in terms of the (period) average location of the zero shear stress point on the wall. Kelvin-Helmholtz vortices evolve along the shear layer and become large enough to be apparent at about 2 step-heights downstream. At Reynolds number of 4000 (calibrated with respect to step height), the shear layer above the recirculation and the reattachment zones typically comprises 4 vortical structures, where the downstream pair merges to form a larger structure. Inasmuch as the number and merging behavior of

large shear layer vortices is concerned, the 2D backward facing step is considerably simpler and more regimented than the free shear layer. Nonetheless, key features, such as asynchronous perturbations, including low frequency modulation of vortex release and merging, are typical in the natural flow.

Large vortical structures cause large-scale entrainment and mixing, a highly desirable effect, e.g. in combustors [15] and in a related configuration, in aggressive diffusers [29]. The objective of actuation is therefore to excite faster shear layer growth to enhance mixing. Reattachment in the natural flow is at about 6 step-heights downstream, whereas the increased stirring motion under open loop actuation, here, using the subharmonic of the natural instability frequency, can bring it to about 4 step-heights. The actuation frequency and amplitude will be denoted ω and A , respectively:

$$a(t) = A \sin(\phi_a), \quad \frac{d}{dt}\phi_a = \omega \quad (1)$$

Previous studies of feedback control of this system at TU Berlin aimed to regulate the reattachment point, using the actuation voltage amplitude as a command signal, and obtaining flow information from an array of (15) pressure gages (microphones) on the floor of the reattachment zone [30], [31]. Here the objective is to refine the control command with flow phase actuation: Simulations of the sinusoidally actuated flow reveal that under open loop actuation the average actuation phase is $\phi \approx -90^\circ$ at the release of a new vortex. Since the flow responds to a destabilizing perturbation by synchronizing its unstable mode with the actuation, this phase coincidence is viewed as optimal for shear growth, and the design objective set forth is to introduce slow corrections into the actuation, to compensate for occasional spontaneous and disturbance driven drifts from this phase relation¹. That is, control design, in this note, concerns slow feedback corrections to the phase dynamics, in (1).

The flow phase is defined by the (nearly) periodic vortex release at the step corner. A dynamic observer, estimating the flow phase, is a critical component in this scheme. As mentioned above an array of microphones is aligned in the stream-wise direction, on the step floor. The microphones provide readings $\mathbf{p}_i(t)$ of the short time pressure fluctuations $\mathbf{p}'_w(t, \mathbf{x})$ (where $\mathbf{x} = (x, y)$ is the location of a point in the 2D section in which the microphones are located). Pressure fluctuations at each point result from the low pressure associated with passing shear layer vortices. Thus, the travelling wave formed by $\mathbf{p}'_w(t, \mathbf{x})$ has a fixed nominal phase relations to shear layer vortices flow and the control objective can be restated in terms of a desired relation between the actuation phase and the phase of that travelling wave, as determined from long term

¹We are content here with a heuristic justification of the chosen design objective, for two reasons: To begin with, it serves the essence of this benchmark study, which is rather to demonstrate the utility of dynamic phasor estimation for phase corrections in nearly periodic flow and actuation, as detailed below. Moreover, while a rigorously found objective could be based, say, on adjoint optimization of a well defined cost function, our criterion is well grounded in basic tenets of fluid mechanics, and its validity in the current context will be demonstrated in experimental results.

average of the sinusoidally actuated flow. Experiments indicate a phase difference of -65° between actuation signal and vortex release, rather than the theoretically predicted -90° .

The following is worth stressing in closing, when viewing this problem from a mainstream control theoretical perspective. The emphasis on “small” and “slow” corrections, above, is judicious, indeed, critical: First, near field vortices are not discernable, and vortex release can be detected only once the vortex has convected and grown downstream. As in any other control system, the presence of measurement delay restricts feasible closed loop bandwidth to time constants that are significantly longer than the convection time of 2-3 periods. Beyond this generic restriction, high bandwidth and high gain actuation can introduce flow structures that deviate significantly from the postulated periodically dominated flow. Given the intrinsic complexity of a fluid flow system, it is hard, if not altogether impossible to predict such dynamics in *any* low order modeling framework, including the phasor models discussed in §III. In addressing fluid flow control, the very intent to design real time feedback based on a low dimensional dynamic representation thus restricts actuation to adhere to the rather limited dynamic repertoire that such a model can cover.

III. OBSERVER AND FEEDBACK FOR THE BACKWARD FACING STEP FLOW

We begin observer design with the simpler of the two benchmarks, the backward facing step. One approach to shear layer observer design is to use a detailed flow model (e.g., a Lagrangian vortex model) and estimate vortex location as a nonlinear inverse problem, as in [27], [32]. Recognizing the potential fragility and sensor requirements of such solutions, the very simple alternative considered here was previously tested in the context of a rotating vortex pair [22]: The temporally and spatially periodic travelling waveform $\mathbf{p}'_w(t, \mathbf{x})$ is ideally represented by a fixed set of Fourier coefficients, or *phasors*. The system model is then reduced to a slow drift in these phasors, driven by a disturbance. Extracting the *innovation signal* from a comparison of sensor readings projection on the waveforms subspace and the predicted waveform is an effective means for filtering pervasive high frequency perturbations and random span-wise dynamics in the flow (i.e., in the orthogonal direction to the crosscut plane of Figure 2).

Following are specific steps in the suggested algorithm. Preprocessing of raw sensor data comprise of the following:

- Microphones capture pressure fluctuations and induce frequency dependent nonlinear phase shift and damping. These effects are calibrated against ideal values of $\mathbf{p}'_w(t, \mathbf{x}_i)$, where \mathbf{x}_i is the i^{th} microphone location.
- In addition to the effect of passing shear layer vortices, pressure fluctuations are caused by external acoustic disturbances and are subject to drift. Both the effect of remote sources and slow drift are characterized by relatively low spatial frequency, hence similar impact on the (calibrated) readings of all sensors. That component is removed by subtracting the calibrated value of one sensor reading from those of all the other sensors.

• Due to vortex growth and shear-layer bending, pressure fluctuations increase in the downstream direction. The envelope varies as a function of changes in the reattachment point, and is determined by a combination of an off-line, long term computation in a preprocessing step, and low-pass real time correction. Sensor readings are normalized by the envelope amplitude, to create readings of an ideal sinusoidal travelling wave. The normalized instantaneous value of the i^{th} sensor are denoted \mathbf{p}_i^n .

The normalized travelling waveform representation of the sensor readings is ideally of the form

$$\begin{aligned} \mathbf{p}_i^n(t) &= R \sin(\phi_w(t) - 2\pi x_i/\lambda) \\ &= R \sin(\phi_a(t) + \phi_d - 2\pi x_i/\lambda) \end{aligned} \quad (2)$$

where $\phi_w(t)$ is defined as the phase of the pressure fluctuation wave form, $\phi_a(t)$ is the actuation phase, as in (1), λ is the spatial period and ϕ_d stands for the *phase difference* between the normalized travelling wave and the actuation. In particular, the nominal natural dynamics are determined by (1) and a postulated constant λ

$$\frac{d}{dt}\phi_w = \omega, \quad \frac{d}{dt}\lambda = 0 \quad (3)$$

The instantaneous spatial Fourier coefficients of the combined sensor readings are

$$\begin{aligned} \alpha(t) &= R \sin(\phi_w(t)) = R \cos(\phi_a(t) + \phi_d) \\ \beta(t) &= R \cos(\phi_w(t)) = R \sin(\phi_a(t) + \phi_d) \end{aligned} \quad (4)$$

and our control objective is stated in terms of a target value ϕ_{d*} for ϕ_d , whether ϕ_{d*} is assigned the ideal value of $\phi_{d*} = 0$ or otherwise.

The need for feedback is due to the possibility (indeed, likelihood) for slow drift in both R , λ and ϕ_d . For example, fluctuations in λ (and R) will result from changes in the mean incoming flow velocity. Other causes include low frequency dynamics in both the span-wise and stream wise directions that are not manifest in low order models. The next processing steps aim to extract measurements of R , λ and ϕ_d from sensor data:

• The instantaneous measurements $\mathbf{p}_i^n(t)$ are projected (using straightforward least mean square approximation) on the spatial harmonic modes $\cos(\frac{2\pi}{\lambda_j}x)$ and $\sin(\frac{2\pi}{\lambda_j}x)$, for an array of wave lengths λ_j , to obtain associated first harmonic spatial Fourier coefficient pairs $(\alpha_j(t), \beta_j(t))$. Using the subscript “ m ” to indicate the value selected as the measured quantity, the instantaneous measured wave length λ_m and the associated measured $(\alpha_j(t), \beta_j(t))$ are those for which the *measured* amplitude $R_m = \sqrt{\alpha_m^2 + \beta_m^2}$ is the largest among $R_j = \sqrt{\alpha_j^2 + \beta_j^2}$. The *measured* oscillation phase is $\phi_m(t) = \angle(\alpha_m(t), \beta_m(t))$.

• Dynamic observers, estimating the values of λ and ϕ , are simple 1st order low pass filters, suppressing high frequency disturbances. Implemented in discrete time these are of the form

$$\begin{aligned} \hat{\lambda}(t_{k+1}) &= (1 - \sigma)\hat{\lambda}(t_k) + \sigma\lambda_m(t_{k+1}) \\ \hat{\phi}_w(t_{k+1}) &= (1 - \rho)(\hat{\phi}_w(t_k) + \Delta t\omega) + \rho\phi_m(t_{k+1}) \end{aligned} \quad (5)$$

where $0 < \sigma, \rho \ll 1$ are the filter coefficients and $\Delta t = t_{k+1} - t_k$ is the time step.

An estimate $\hat{\mathbf{p}}'_w(t, \mathbf{x})$ of the distributed pressure fluctuations can now be obtained by reversing the normalization step, using R_m (or a low pass filtered version) and the estimated $\hat{\lambda}$ and $\hat{\phi}_w$ in (2). That estimate, however, is unnecessary. The practical aspect of the estimation is the correction for drift in ϕ_d in the actuation:

• The actuation phase at the time t_k is determined by the estimated phase of the sensor signal wave form and the designated ϕ_{d*} .

$$\phi_a(t_k) = \hat{\phi}_w(t_k) + \phi_{d*}. \quad (6)$$

Experimental Results. The algorithm was implemented in the testbed in Figure 2. Results are depicted in Figure 3. The plot compares the period average of the reattachment point x_R , normalized by the reattachment length of the natural flow, under open (red line) and closed loop actuation (marked points at selected ϕ_d). Three closed loop experiments were conducted with different selection of the low pass filter of the wave form Fourier coefficients. The efficiency of the actuation can be increased by forcing $\phi_d > 0$, thus effectively increasing the frequency slightly. The reverse effect is achieved by enforcing $\phi_d < 0$.

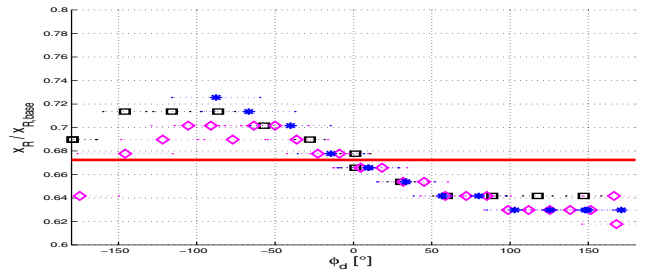


Fig. 3. Wind tunnel experiments with the backward facing step flow. Comparison of the period average of the reattachment point x_R , normalized by the reattachment length of the natural flow. The effect of open loop actuation (red line) is compared to closed loop actuation, as a function of the selected ϕ_d (marked points). Three closed loop experiments were conducted with different selection of the low pass filter of the wave form Fourier coefficients. (Black squares: fast adaptation with a time constant of $\tau = 0.05T$, where T is the actuation period, magenta diamonds: $\tau = 0.2T$, asterisk: $\tau = 0.5T$). $\phi_d > 0$ increases, $\phi_d < 0$ decreased the efficiency of the actuation compared to open loop. The tracking capability of the observer deteriorates at very high and very low ϕ_d , respectively. This puts a limit to both increase and decrease of efficiency.

IV. A FREE SHEAR LAYER OBSERVER

Here we highlight features added to the previous case, to address the presence of asynchronous vortex merging. The sampled trajectory of velocity measurements is denoted $\mathbf{u}_m(t) = (u_m(t), (x_i, -15))_i$, and the observer estimates the x -coordinates of shear layer vortices.

The Near Field Shear Layer ($0 \leq x \leq 4\lambda$): Vortices do not merge and maintain the time frequency ω , spatial wave length λ , and convection velocity of U_s .

• The $[0, 4\lambda]$ component of \mathbf{u}_m forms a single harmonic travelling wave. Its spatio-temporal Fourier coefficients are

ideally constants. Dynamic corrections are obtained by the low pass filtered deviation between the coefficients of the projected instantaneous wave form and previous estimates. The used filter time constant is $0.67T$.

- Stream-wise velocity below the shear layer is negative. Local minima indicate passing vortices. Measured locations of local minima are easily extracted from the reconstructed single (first) harmonic wave form.

- As a vortex estimate reaches $x = 4\lambda$, it is handed over to the downstream observer and a new upstream vortex location is estimated at $x = 0$.

The Downstream Shear Layer ($4\lambda \leq x \leq 14\lambda$): Estimation of individual vortex locations becomes local and the convection velocity varies between vortices due to the effect of paired vortices and varying distances between them. The dynamic estimates for each vortex therefore includes *both* the position \hat{x}_i and convection velocity \hat{u}_i , initiated at 4λ and U_s , respectively. Measured corrections, as described below, are low pass filtered with a long time constant.

- A vortex pair is merged and the estimator for one of the two is removed once their estimated horizontal distance reduces below a tolerance $\eta = 2 = 0.1\lambda$.

- We distinguish between several cases, relating to the position and convection velocity of the i^{th} vortex:

- If the $i + 1^{st}$ vortex is a merged (double) vortex, its effect on sensor readings is typically larger than that of the i^{th} vortex, excluding the search for- and use of the location of a local minimum in the measured fluid velocity below the i^{th} vortex. The $i + 1^{st}$ vortex has an accelerating effect on the i^{th} vortex. A very simple way to correct for that effect is as follows: At the time t_{k+1} , the sensor readings over the interval $[\hat{x}_i(t_k), \hat{x}_i(t_k) + 2\lambda]$ are projected over the 1^{st} spatial subharmonic. The located minimum of this waveform indicates a point \bar{x}_{i+1} of maximal effect of the merged vortex. This position is used as a low pass filtered update for the next position: $\hat{x}_i(t_{k+1}) = (1 - \nu)\hat{x}_i(t_k) + \nu\bar{x}_{i+1} + \hat{u}_i(t_k) \cdot \Delta t$, with the corresponding update on the convection velocity. A long filter time constant of $8T$ was used.

- Else, the second harmonic expansion of sensor signals is evaluated over the interval $[\hat{x}_i(t_k) - 0.25\lambda, \hat{x}_i(t_k) + 0.25\lambda]$. If this expansion attains a minimum over $[\hat{x}_i(t_k) - 0.125\lambda, \hat{x}_i(t_k) + 0.125\lambda]$, that minimum will be used as a new measured position, and low pass filtered (with a time constant of $0.8T$) to update both $\hat{x}_i(t_{k+1})$ and $\hat{u}_i(t_{k+1})$. Sharper minima due to the presence of paired vortices motivates the use of the 2^{nd} harmonic.

- Else, the first harmonic expansion of sensor signals is evaluated over the interval $[\hat{x}_i(t_k) - 0.5\lambda, \hat{x}_i(t_k) + 0.5\lambda]$. If this expansion attains a minimum over $[\hat{x}_i(t_k) - 0.25\lambda, \hat{x}_i(t_k) + 0.25\lambda]$, it will be used as a measured position in updates, as above.

- If no local minimum is found, no velocity update is applied: $\hat{u}_i(t_{k+1}) = \hat{u}_i(t_k)$ and $\hat{x}_i(t_{k+1}) = \hat{x}_i(t_k) + \hat{u}_i(t_{k+1}) \cdot \Delta t$.

Figure 4 depicts two generic snapshots of the vorticity dis-

tribution in the flow and dynamic estimates of the locations of vortical structures. The figure illustrates both near field shear layer vortex tracking and a reasonable ability to continue tracking vortices as they aggregate into larger structures. Some local estimation distortions are due to the effect of variations in the vertical vortex positions on the measured velocity. These variations are not accounted for in the simple model used here, illustrating the potential advantages of including more details, such as using a Biot-Savart equation in the context of aggregated vortices, as a forward model in a dynamic inverse problem solution.

V. CONCLUDING REMARKS

A proposed simple observer structure, estimating vortex locations along a shear layer from an array of velocity or pressure sensors is based on a phenomenological dynamic phasor model for the travelling waveform of sensors' readings. The dynamic estimate provides phase information that enables harmonic corrections in a periodic actuation signal, in order to manipulate - and increase - shear layer growth, with beneficial effects on mixing. The observer is illustrated in both simulations and closed loop control experiments for the flow over a backward facing step, and in an ideal free shear layer simulations.

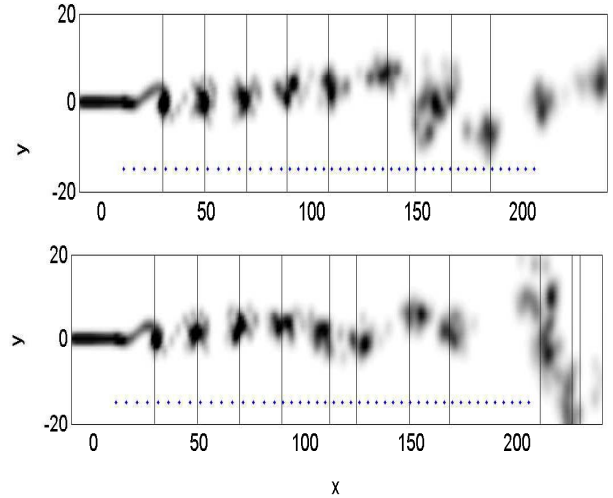


Fig. 4. Snapshots of the vorticity distribution and vortical structures tracking in the free shear layer. Dark spots indicate high vorticity. Vertical lines are estimates of vortex location and blue dots along $y = -15$ indicate velocity sensors. Estimates downstream of the last sensor not updated and eventually abandoned. Thus, no estimate is provided for the locations of the two downstream-most structures.

REFERENCES

- [1] G. K. Batchelor. *An Introduction to Fluid Dynamics*. Cambridge University Press, Cambridge, 1967.
- [2] J. M. Ottino. Unity and diversity in mixing - stretching, diffusion, breakup, and aggregation in chaotic flows. *Physics of Fluids A*, 3:1417–1430, 1991.
- [3] M. Gad el Haq and D. M. Bushnell. Separation control: Review. *ASME J. Fluids Eng.*, 113(5): , 1991.
- [4] J. O. Keller, T. T. Bramlette, P. K. Barr, and J. R. Alvarez. NO_x and CO emissions from a pulse combustor operating in a lean premixed mode. *Combuster and Flame*, 99:460 – 466, 1994.
- [5] S. Ghosh, A. Leonard, and S. Wiggins. Diffusion of a passive scalar from a no-slip boundary into a chaotic advection field. *J. Fluid Mech.*, 1998.

- [6] T. R. Bewley. Flow control: new challenges for a new renaissance. *Progress in Aerospace Sciences*, 37:21 – 58, 2001.
- [7] M. Gunzburger. *Perspectives in Flow Control and Optimization*. SIAM, 2002.
- [8] O. Aamo and M. Krstic. *Flow Control by Feedback Stabilization and Mixing*. Springer, 2003.
- [9] R. M. Murray (Editor). *Control in an Information Rich World: Future Directions in Control, Dynamics, and Systems*. SIAM, 2003.
- [10] L. Cattafesta, D.R. Williams, C.W. Rowley, and F. Alvi. Review of active control of flow-induced cavity resonance. In *33rd AIAA Fluid Dynamics Conference*, 2003. AIAA paper 2003-3567.
- [11] Y.K. Suh. Periodic motion of a point vortex in a corner subject to a potential flow. *J. Phys. Soc. Jap.*, 62(10):3441–3445, 1993.
- [12] D. Vainchtein and I. Mezić. Control off a vortex pair using weak external flow. *J. of Turbulance*, 3:51, 2002.
- [13] F. Li and N. Aubry. Feedback control of flow past a cylinder via transverse motion. *Physics of Fluids*, 15:2163–2176, 2003.
- [14] M. Pastoor, R. King, B.R. Noack, A. Dillmann, and G. Tadmor. Model-based coherent-structure control of turbulent shear flows using low-dimensional vortex models. In *33rd AIAA Fluids Conference and Exhibit*, Orlando, Florida, U.S.A., June 23–26, 2003, 2002. Paper 2003-4261.
- [15] B.R. Noack, I. Mezić, G. Tadmor, and A. Banaszuk. Optimal mixing in recirculation zones. *Phys. Fluids*, 16(4):867–888, 2004.
- [16] B. Protas. Linear feedback stabilization of laminar vortex shedding based on a point vortex model. *Phys. Fluids*, 16(12):4473–4488, 2004.
- [17] B.R. Noack, K. Afanasiev, M. Morzyński, G. Tadmor, and F. Thiele. A hierarchy of low-dimensional models for the transient and post-transient cylinder wake. *J. Fluid Mech.*, 497:335–363, 2003.
- [18] B.R. Noack, P. Papan, and P.A. Monkewitz. The need for a pressure-term representation in empirical Galerkin models of incompressible shear flows. *J. Fluid Mech.*, 523:339–365, 2005.
- [19] C.L. DeMarco and G.C. Verghese. Bringing phasor dynamics into the power system load flow. In *North American Power Symposium*, pages 463–469, 1993.
- [20] G. Tadmor. On approximate phasor models in dissipative, bilinear systems. *IEEE Transaction on Circuits & Systems I: Fundamental Theory*, 49:1167 – 1179, 2002.
- [21] G. Tadmor and A. Banaszuk. Observation feedback control of vortex motion in a recirculation region. *IEEE Transactions on Control Systems Technology*, 10:749 – 755, 2002.
- [22] G. Tadmor. Observers and feedback control for a rotating vortex pair. *IEEE Transactions on Control Systems Technology*, 12:36 – 51, 2004.
- [23] A. Michalke. On spatially growing disturbances in an inviscid shear layer. *J. Fluid Mechanics*, 23:521 – 544, 1965.
- [24] P.G. Drazin and W.H. Reid. *Hydrodynamic Stability*. Cambridge University Press, 1981.
- [25] R. R. Ruderich and H.H. Fernholz. An experimental investigation of a turbulent shear flow with separation, reverse flow and reattachment. *J. Fluid Mechanics*, 163:283–322, 1985.
- [26] M.A.Z. Hasan. The flow over a backward-facing step under controlled perturbation: laminar separation. *J. Fluid Mechanics*, 238:73–96, 1992.
- [27] T. Suzuki, T. Colonius, and D. G. MacMartin. Inverse technique for vortex imaging and its application to feedback flow control. In *33rd AIAA Fluid Dynamics Conference*, June 2003. AIAA-2003-4260.
- [28] T. Weinkauf, H.-C. Hege, B.R. Noack, M. Schlegel, and A. Dillmann. Coherent structures in a transitional flow around a backward-facing step. *Phys. Fluids*, 15(9):S3, 2003.
- [29] B. Collier, B. R. Noack, S. Narayanan, A. Banaszuk, and A. I. Khibnik. Reduced basis model for active separation control in a planar diffuser flow. In *AIAA, Fluids 2000, Denver*, 2000. paper 33894.
- [30] R. Becker, M. Garwon, and R. King. Development of model-based sensors and their use for closed-loop control of separated shear flows. In *Proceedings of the European Control Conference*, University of Cambridge, UK, September 1–4, 2003, 2003.
- [31] R. King, R. Becker, M. Garwon, and L. Henning. Robust and adaptive closed-loop control of separated shear flows. In *2nd AIAA Flow Control Conference*, Portland, Oregon, U.S.A., 28.6.–1.7.2004, 2004. Paper 2004-2519.
- [32] T. Suzuki and T. Colonius. Inverse-imaging method for detection of a vortex in a channel. *AIAA J.*, 41:1743–1751, 2003.

Acknowledgement. We acknowledge funding of the Deutsche Forschungsgemeinschaft (DFG), Germany, and the National Science Foundation (NSF), United States. DFG support was via the Collaborative Research Center (Sfb 557) “Control of complex turbulent shear flows” at the Berlin University of Technology and by the grants No. 258/1-1 and DI 448/5-1. NSF support was via grants No. 0136404, 0410246 and 0230489.